Global and Planetary Change 135 (2015) 38–46

Contents lists available at ScienceDirect

Global and Planetary Change

journal homepage: www.elsevier.com/locate/gloplacha

Geochemical evidence for intermediate water circulation in the westernmost Mediterranean over the last 20 kyr BP and its impact on the Mediterranean Outflow

F.J. Jiménez-Espejo [a,*], M. Pardos-Gené [b], F. Martínez-Ruiz [b], A. García-Alix [c], T. van de Flierdt [d], Takashi Toyofuku [e], Andre Bahr [f], Katharina Kreissig [d]

[a] Department of Biogeochemistry, Japan Agency for Marine-Earth Science and Technology (JAMSTEC), Yokosuka 237-0061, Japan
[b] Instituto Andaluz de Ciencias de la Tierra (CSIC), Avenida de las Palmeras 4, 18100 Armilla, (Granada), Spain
[c] Department of Geographical and Earth Sciences, University of Glasgow, UK
[d] Department of Earth Science and Engineering, Imperial College London, South Kensington Campus, Prince Consort Road, London SW7 2AZ, UK
[e] Department of Marine Biodiversity Research (Bio-dive), Japan Agency for Marine-Earth Science and Technology (JAMSTEC), Yokosuka 237-0061, Japan
[f] Institute of Earth Sciences, Heidelberg University, Heidelberg, Germany

ARTICLE INFO

Article history:
Received 2 March 2015
Received in revised form 1 September 2015
Accepted 6 October 2015
Available online 23 October 2015

Keywords:
Alboran basin
Levantine Intermediate Water
Last Glacial cycle
Nd isotopes
Redox conditions
Mediterranean Outflow

ABSTRACT

The Mediterranean Outflow (MOW) is generated by deep and intermediate waters from different basins in the Mediterranean Sea. Despite the number of studies on Mediterranean water masses, little work has been done on the source and properties of intermediate waters in the westernmost Mediterranean Sea and their links with MOW. Here we examine three marine sediment records spanning the last 20 kyr, located at key depths to trace intermediate waters along the Alboran Sea. We use a combination of redox-sensitive elements, which can serve as proxies to reconstruct variations in the water column oxygenation and the Nd isotopic composition of foraminiferal ferromanganese coatings, in order to reconstruct water mass provenance of Eastern/Western Mediterranean waters. As measured, $\varepsilon_{Nd} < -9.2$ and a low U/Th ratio during glacial periods can be attributed to the presence of Western Mediterranean Deep Water (WMDW) at the study sites. During deglaciation, higher Nd isotopic compositions and U/Th ratios point to an enhanced contribution of the modified Levantine Intermediate Water (LIW). The comparison between our data and other LIW and MOW records suggests that i) the lower branch of MOW is linked to WMDW during the glacial period, ii) the middle MOW branch follows LIW activity during deglaciation, while iii) the upper branch is more active during late Holocene, coinciding with LIW formation increase after sapropel deposits. This reconstruction has significant implications for an understanding of the MOW evolution.

1. Introduction

The Mediterranean Sea is connected with the northeastern Atlantic Ocean through the Strait of Gibraltar. The Mediterranean Outflow Water (MOW) has a strong impact on the composition of North Atlantic intermediate waters, hence playing an important role in global thermohaline circulation (Johnson, 1997; Sierro et al., 2005; Rogerson et al., 2006; Hernandez-Molina et al., 2014; Ivanovic et al., 2014). A strong MOW input has been associated, for example, with the recovery of the Atlantic thermohaline circulation after the Last Glacial Maximum (e.g., Rogerson et al., 2006; Voelker et al., 2006). At present, the MOW is predominantly fed by intermediate and deep Mediterranean waters (Bryden and Stommel, 1984).

A key location for understanding MOW is the Alboran Sea, within the westernmost Mediterranean. Most previous studies involving the Alboran Sea (e.g., Barcena et al., 2001; Cacho et al., 2001; Martrat et al., 2004; Moreno et al., 2005; Jimenez-Espejo et al., 2007; Rohling et al., 2015 and references therein) focus on reconstructing surface water and deep water conditions, while information about intermediate waters remains scarce. Yet compared to surface and deep water masses, intermediate waters display distinct hydrographic features (e.g. Font, 1987; Millot, 2009), and a very characteristic geochemical fingerprint (e.g. their Nd isotopic composition; Tachikawa et al., 2004).

A key open question is how to reconstruct the source and properties of Mediterranean intermediate waters and their relationship with the MOW. In studying relative water mass contributions to the MOW during the last deglaciation and the Holocene, we deploy a range of geochemical proxies on three sediment records recovered in the Alboran Sea basin. The cores are located at depths between 1800 and

* Corresponding author.
E-mail addresses: fjjspejo@jamstec.go.jp (F.J. Jiménez-Espejo), mpardos@iact.ugr-csic.es (M. Pardos-Gené), Antonio.Garcia-AlixDaroca@glasgow.ac.uk (A. García-Alix), tina.vandeflierdt@imperial.ac.uk (T. van de Flierdt), toyofuku@jamstec.go.jp (T. Toyofuku), andre.bahr@geow.uni-heidelberg.de (A. Bahr), k.kreissig@imperial.ac.uk (K. Kreissig).

http://dx.doi.org/10.1016/j.gloplacha.2015.10.001
0921-8181/

2400 mbsf, allowing for an intermediate/deep water mass reconstruction (De Lange et al., 2008; Tachikawa et al., 2015). The utilized proxies include the Nd isotopic composition of seawater as a quasi-conservative water mass proxy, as well as redox sensitive trace elements to constrain the redox conditions in the water column. Our new data may provide novel insights into the evolution of Levantine Intermediate Water (LIW) and Mediterranean thermohaline circulation, leading to an improved understanding of the MOW over time.

1.1. Oceanographic setting

The general circulation in the Mediterranean is a result of high evaporation rates and MOW activity (Ovchinnikov et al., 1976; Millot, 2009; MerMex Group et al., 2011). In the Western Mediterranean Sea (WMS), three main water masses can be distinguished: Modified Atlantic Water (MAW), Levantine Intermediate Water (LIW), and Western Mediterranean Deep Water (WMDW). The MAW forms as a result of the comparatively fresh Atlantic water ($S < 36.5$) entering the Mediterranean Sea via the strait of Gibraltar and mixing with the surface waters of the Alboran Sea. The MAW flows eastward as a 150–200 m thick surface layer.

On the other hand, the LIW originates in the Eastern Mediterranean Sea (EMS) through sinking during winter times (Cramp and O'Sullivan, 1999) and can be identified in the study area at depths between 200 and 600 m. Finally, WMDW is found below this water depth, being generated by surface cooling in the Gulf of Lion. Its main flow path is along the Moroccan margin (Hernandez-Molina et al., 2002).

The MOW comprises a mixture of these deep and intermediate water masses (Parrilla et al., 1986; Millot, 1999) (Figs. 1 and 2). Its formation has been related to the wind strength, predominant circulation patterns of source waters, freshwater input, temperatures and the density of surface waters, among other factors (e.g., Rohling and Bryden, 1992; Bethoux et al., 1998; Cramp and O'Sullivan, 1999; Millot, 2009).

2. Materials and methods

2.1. Site description and age model

We obtained our data from Sites 300G, 302G and 304G, situated at different depths (1860 m, 1989 m, and 2382 m, respectively; Table 1) along the west–east trending East Alboran basin slope; they are currently bathed in the WMDW (Figs. 1 and 2). The incoming MAW flow generates a quasi-permanent anticyclonic gyre in the western Alboran Sea and a transient gyre at the eastern part of the basin (Fig. 1). The hydrological front is characterized by a strong horizontal density gradient (>0.4 kg m^3) between MAW and the LIW (Tolosa et al., 2003).

Age models for the three sites have been published previously (Jimenez-Espejo et al., 2008) and are based on monospecific planktonic foraminifera ^{14}C-AMS dates (accelerator mass spectrometry), stable isotope stratigraphy, and the correlation of geochemical elemental ratio profiles among sites. The cores span the past 20 kyr BP (Table 1) and were collected during Training-Through-Research (TTR) Cruise 14 in order to track shifts in the water column structure. Recovered lithologies comprise homogenous grayish olive nannofossil clay and nannofossil-rich silty clay (Comas and Ivanov, 2006). The studied intervals and their detrital elemental composition show no indication of grain-sorting processes, indicative of strong bottom currents, or turbiditic sequences (Jimenez-Espejo et al., 2008). Sedimentation rates in the Alboran basins range from approximately 10 cm/ka during the late Holocene up to 20 cm/kyr during some pre-Holocene periods. Sampling resolution was 3 cm at site 300G and between 3 and 7 cm at sites 302 and 304, yielding a temporal resolution of ~200 to ~500 yrs. depending on site and time interval.

2.2. Methods

Major element concentrations (Fig. 3) were obtained by atomic absorption spectrometry (AAS) (Perkin-Elmer 5100 spectrometer), with an analytical error of 2%, at the Instituto Andaluz de Ciencias de la Tierra (CSIC-UGR). Analysis of trace elements (U, Th and Ba) was performed using inductively coupled plasma-mass spectrometry (Perkin-Elmer Sciex Elan 5000 ICP-MS) following HNO_3 + HF digestion. Measurements were carried out as triplicates using Re and Rh as internal standards at the Centro de Instrumentación Científica (University of Granada). External reproducibility was determined by dissolving 10 replicates of powdered samples and results were in agreement within 3% for analyte concentrations of 50 ppm and within 8% for analyte concentrations of 5 ppm (Bea, 1996). From the suite of analyzed major and trace elements, U, Th and Ba (and corresponding normalized concentrations) were selected as proxies for water mass reconstructions.

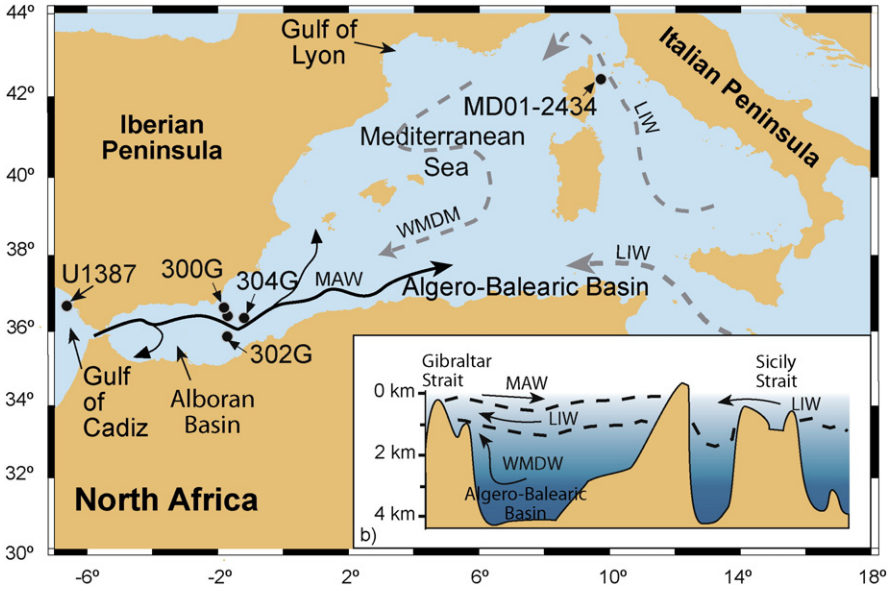

Fig. 1. a) Map of the western Mediterranean Sea with setting of studied gravity cores 300G, 302G and 304G in the Alboran Sea. Also shown are sites IODP-U1387 and MD01-2434 for comparison. Black and dashed gray lines represent the flow directions of major water masses, Western Mediterranean Deep Water (WMDW), Levantine Intermediate Water (LIW) and Modified Atlantic Water (MAW). b) Cross-section showing water mass stratification in the Mediterranean. Modified from Cramp and O'Sullivan (1999).

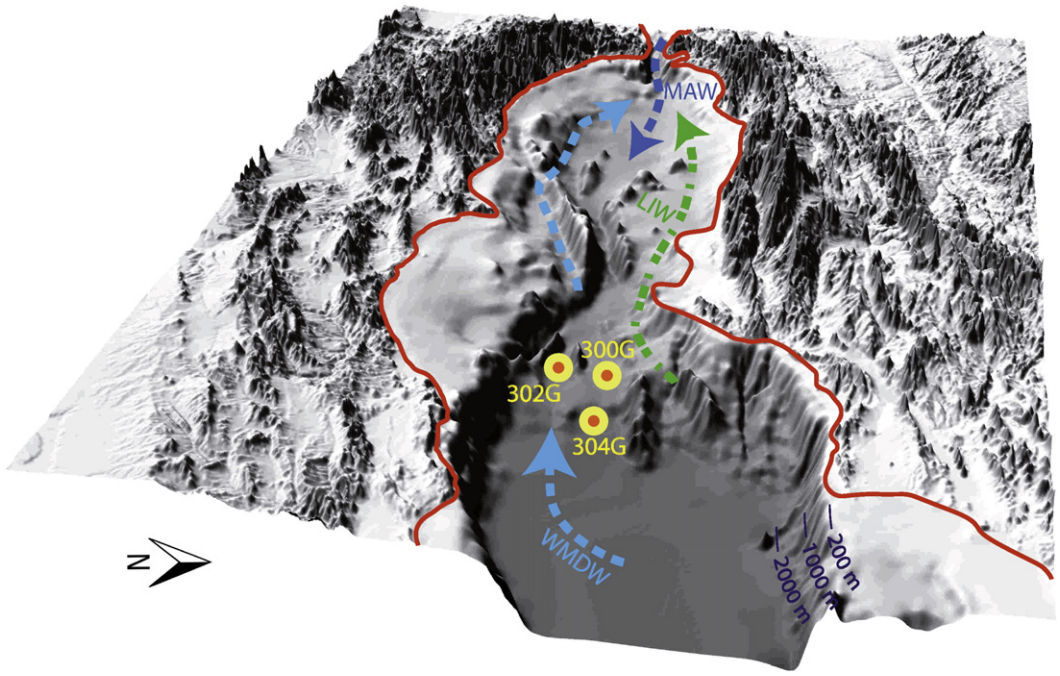

Fig. 2. Gibraltar Strait and Alboran basin bathymetry and raised-relief maps with vertically exaggerated scale viewed from the East. Dashed lines represent the pathways of the main currents in the area (modified from Hernandez-Molina et al., 2002). Modified Atlantic Water (dark blue), Levantine Intermediate Water (green), and Western Mediterranean Deep Water (light blue). Red line represents the coast line.

Authigenic Nd isotopic compositions of bottom waters were reconstructed based on the Fe-Mn oxide coatings around foraminifera tests in the MAGIC laboratories at Imperial College, London, following the pioneering work of Roberts et al. (2010) (Table 2). Briefly, ~80 mg of planktonic foraminifera were picked from the >125 μm fraction of 11 sediment samples from two different core sites (304G and 302G) located in the western gyre of the Alboran Sea. Sampled tests were crushed between glass plates, ensuring that all chambers were opened. Thereafter, samples were ultrasonicated in glass beakers (with 5 ml de-ionized water) for ~1 min before pipetting off the waste water. This step was repeated until the water was clear (i.e., no clay left). The cleanliness of samples was checked under a microscope and visible pieces of pyrite and detrital particles were removed. Digestion of foraminifera was achieved by addition of 1 ml of 1 M acetic acid.

Additionally, four samples from sites 302G and 304G were investigated for their detrital Nd isotopic composition following sequential extraction of authigenic carbonate and ferromanganese coatings as described previously (see Biscaye, 1965; Rutberg et al., 2000) (Table 2). ~50 mg of detrital material was digested on a hotplate using a mixture of 0.5 ml 20 M $HClO_4$, 1 ml 15 M HNO_3 and 3 ml 27 M HF. After conversion to nitrate form, Nd was separated from the sample matrix and other rare earth elements by means of two-step ion chromatography (TRU-spec and Ln-spec columns; modified after Pin and Zalduegui, 1997). Neodymium isotope measurements were carried out on a Nu Plasma-HR MC-ICPMS. Instrumental mass bias was corrected for using a $^{146}Nd/^{144}Nd$ ratio of 0.7219 and an exponential law. Samarium interferences were monitored and were significantly below the correctable level of 0.1% ^{144}Sm on ^{144}N in all samples. Repeated analyses of the JNdi-1 standard yielded values of 0.512107 ± 0.000014, 0.512133 ± 0.000015, 0.512121 ± 0.000014, and 0.512072 ± 0.000011 (2sd) over the course of the four days of sample analyses. All sample results are reported relative to a JNdi-1 $^{143}Nd/^{144}Nd$ value of 0.512115 (Tanaka et al., 2000).

3. Paleoenviromental proxies

3.1. Neodymium isotopes as water mass proxies

Neodymium isotope ratios in seawater are often used in paleoceanography as a quasi-conservative tracer of water masses (e.g., Frank et al., 2002; Goldstein and Hemming, 2003). Neodymium isotopes are expressed as ε_{Nd} and denote the deviation of a measured $^{143}Nd/^{144}Nd$ ratio from the Chondritic Uniform Reservoir (CHUR) in parts per 10,000 (present day CHUR = 0.512638; Jacobsen and Wasserburg, 1980). Geological heterogeneity in the continents and their subsequent erosion and delivery to the ocean, as well as exchange of seawater with the ocean margins, leave distinct Nd imprints on water masses, which can be traced spatially due to the short residence time of Nd in the seawater (~400 years; Tachikawa et al., 2003). Modern seawater Nd isotopic compositions range from values as low as $\varepsilon_{Nd} < -20$ in the Labrador Sea, which is surrounded by old continental crust, to values as high as ε_{Nd} ~0 in the North Pacific, close to young volcanic inputs (see Lacan et al., 2012; Jeandel et al., 2007 for an overview). The origin and significance of ε_{Nd} in the Mediterranean Sea has been previously explored, indicating that LIW has an isotopic signature of ε_{Nd} ~−5 in the EMS (Tachikawa et al., 2004; Vance et al., 2004). However, this value becomes less radiogenic in the WMS, where ε_N values $_d$ of ~−8.9 are observed at LIW depths (Henry et al., 1994; Tachikawa et al., 2004). LIW

Table 1
Core data including location, water depth, studied interval and linear sedimentation rates.

Core	Location	Water depth (m)	Studied interval (cm)	Linear sedim. rate (cm/kyr)
TTR14-300G	36° 21,532 N, 1° 47,507 W	1860	266	13.3
TTR14-302G	36° 01,906 N, 1°57,317 W	1989	335	16.75
TTR14-304G	36° 19,873 N, 1° 31,631 W	2382	291	14.55

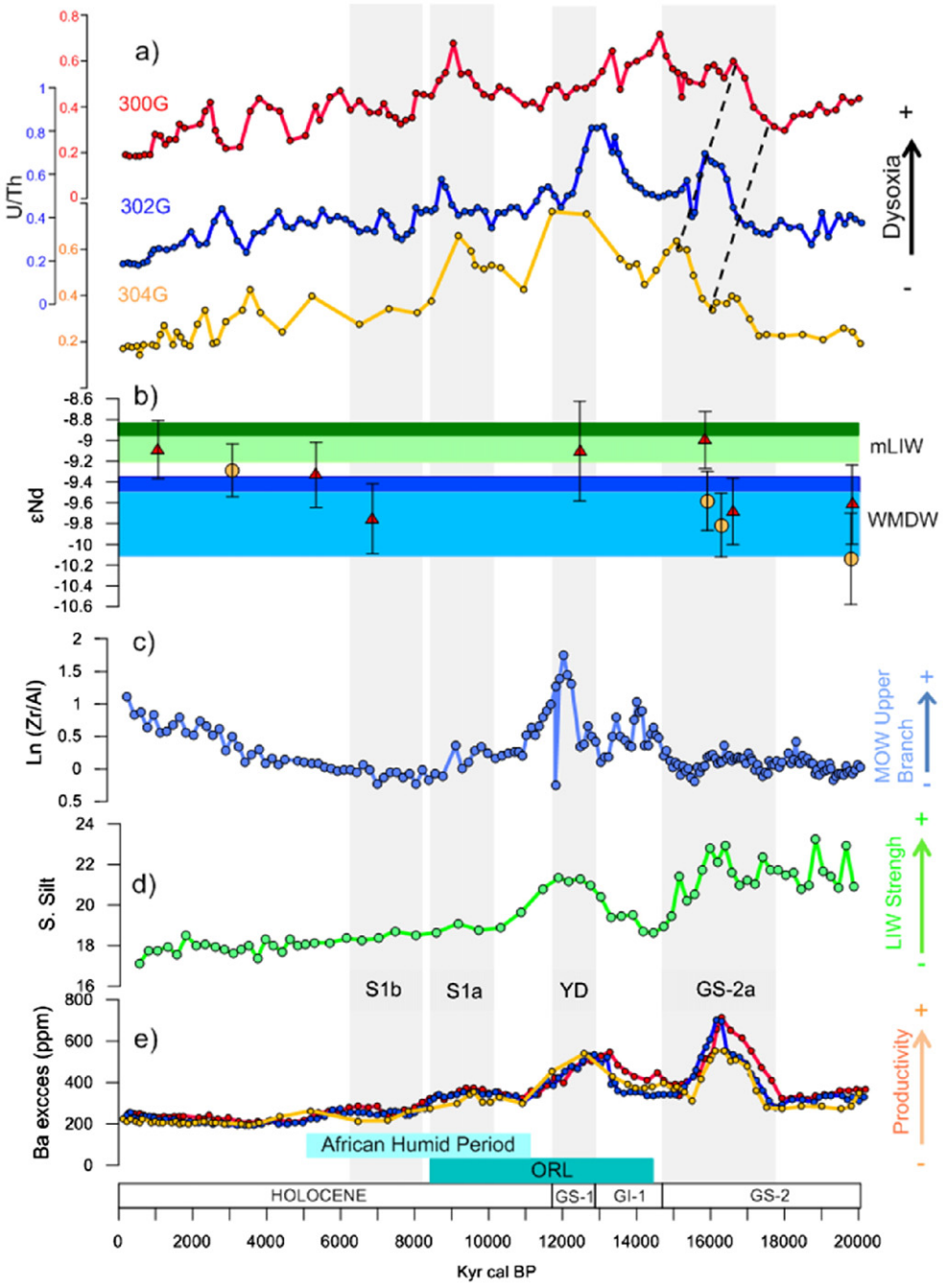

Fig. 3. Time series of geochemical proxies for studied sites TTR-300G, TTR-302G, and TTR-304G from the Alboran Sea (this study) in comparison to previously published records from the area. a) U/Th ratios for sites 300G (red), 302G (blue) and 304G (orange), used as a proxy for the degree of anoxia. b) Neodymium isotope composition of planktonic foraminifera ferromanganese coatings at sites 302G and 304G used as a water mass provenance indicator. Green and blue dark bands respectively display the main range of seawater Nd isotopic compositions of modified Levantine Intermediate Water (mLIW) (εNd ~−8.9, Tachikawa et al., 2004) and the West Mediterranean Deep Water (WMDW) (εNd ~−9.4, Tachikawa et al., 2004). Extended light green and blue bands denote full values range. c) Ln Zr/Al ratio at site U1387 (Gulf of Cadiz), an upper MOW intensity proxy (Bahr et al., 2014). d) Sortable Silt content at site MD01-2434, an LIW intensity proxy (Toucanne et al., 2012). e) Barium excess (ppm) age plotted comparison among cores (Jimenez-Espejo et al., 2008). Light blue bars across the Figure indicate the African Humid Period and the last Organic Rich Layer (ORL) deposited in the Western Mediterranean. Light gray bars indicate Greenland Stadials 2a, Sapropel S1a and S1b (Ariztegui et al., 2000).

reaches these values after crossing the strait of Sicily. Hereafter we will refer to this signature at intermediate depths in the WMS as modified LIW (mLIW). Less radiogenic values are characteristic of WMDW ($\varepsilon_{Nd} = -9.4$; Henry et al., 1994; Tachikawa et al., 2004), the least radiogenic values being recorded in MAW ($\varepsilon_{Nd} \cong -10.4$; Spivack and Wasserburg, 1988; Tachikawa et al., 2004) (Fig. 3). When interpreting the Nd isotopic composition of seawater as derived from authigenic phases in sediments, it should be noted that intense sediment reworking and along-slope transport may alter the use of Nd isotopes as a water mass proxy (e.g., Gutjahr et al., 2008). The Gulf of Cadiz is one such area (Stumpf et al., 2010), though contourites are not described in the eastern Alboran region (Palomino et al., 2011); hence we are confident that Nd isotopes can reliably trace water masses.

3.2. U as paleoceanographic proxy

Uranium in sediments can be hosted in solid phases such as detrital lithogenic components (physically transported to and deposited at the

Table 2
Nd isotopic compositions of foraminiferal coatings and bulk sediments from studied sites. (a) Measured Nd isotopic composition normalized to JNdi $^{143}Nd/^{144}Nd$ value of 0.512115 (Tanaka et al., 2000). JNdi results for the four measurement sessions are reported in the main text. (b) Internal 2σ standard error of the measurements. (c) εNd values are calculated relative to a CHUR value of 0.512638 (Jacobsen and Wasserburg, 1980). (d) External errors are the 2σ deviations derived from repeat analysis of the JNdi standard during the measurement sessions at similar concentrations to sample sizes (10–20 ng Nd). Uncertainties plotted in Fig. 3 are internal 2σ standard errors.

Lab. code	Sample ID	Depth [cm]	Age [yrs]	$^{143}Nd/^{144}Nd$ (a)	2σ SE (b)	ε_{Nd} (c)	2σ SD (d)
Foraminiferal coatings							
302-1	302G 01 12–13.5	14.25	1070	0.512172	0.000016	-9.09	0.28
302-2	302G-02 22.5–24	74.25	5340	0.512160	0.000016	−9.33	0.27
302-3	302G 02 49.5–51	101.25	6870	0.512138	0.000020	−9.75	0.27
302-4	302G 04 42–43.5	204.75	12,478	0.512171	0.000025	−9.10	0.27
302-5	302G 06 04.5–06	273.75	15,870	0.512177	0.000015	−9.00	0.27
302-6	302G 06 19.5–21	288.75	16,620	0.512142	0.000018	−9.68	0.27
302-7	302G 07 07.5–09	332.25	19,844	0.512145	0.000020	−9.62	0.29
304-1	304G 01 40.5–42	41.25	3080	0.512162	0.000013	−9.29	0.22
304-4	304G 04 43.5–45	218.25	15,930	0.512147	0.000015	−9.58	0.22
304-5	304G 04 52.5–54	227.25	16,300	0.512135	0.000012	−9.81	0.27
304-6	304G 05 54–55.5	288.75	19,810	0.512118	0.000023	−10.14	0.27
Bulk sediments							
302 EH	302G 01 16.5–18	18.75	1284	0.511988	0.000010	−12.67	0.28
302 LH	302G 06 24–25.5	293,25	16,780	0.511981	0.000010	−12.82	0.28
304EH	304G 01 23–24.5	23.25	1760	0.511988	0.000009	−12.67	0.28
304 LH	304G 04 48–49.5	164.25	16,130	0.511991	0.000008	−12.62	0.28

site), in authigenic phases (associated with biogenic carbonate and organic biomass), or be derived from reductive authigenic pore-water precipitation (Andersen et al., 2014).

Because U concentrations in the sediment might be further biased by detrital input, the U/Th ratio is used. Normalization of trace element contents to an immobile element — usually Al or Th — is common in paleoceanographical studies, and a vast literature on geochemical proxies demonstrates the usefulness of this ratio (e.g., Van der Weijden, 2002; Calvert and Pedersen, 2007). In this sense, the U/Th ratio allows for correcting the dilution by sedimentary phases barren of a particular trace element. The U/Th ratio thus represents the excess of U with respect to Th (aluminosilicate fraction). The subtraction of the detrital influence on trace elements concentrations is an important issue discussed by different authors (e.g., Chase et al., 2001; Tribovillard et al., 2006; Andersen et al., 2014). Hence, it is important to distinguish whether uranium enrichment is linked to bottom water oxygenation and/or organic matter oxidation and consequent post-depositional sediment reduction forcing U deposition from pore waters (when pore-water nitrate vanishes in sediments beneath the redoxcline, U^{+6} is reduced to immobile U^{+4} and precipitates; Anderson, 1982; Barnes and Cochran, 1990; Mangini et al., 2001). Although the specific behavior of U under oxic and suboxic conditions remains poorly understood, an increase in U deposition has been observed in suboxic basins with respect to oxidized conditions (Andersen et al., 2014). In the WMS, the last organic rich layer (ORL 1, between 14.5 and 8.2 ka) has been associated with the occurrence of sluggish bottom waters (Rogerson et al., 2006). U/Th enrichment is observed for sediments deposited during this ORL interval, and partially the GS-2a period, when Ba based proxies also support enhanced productivity (Fig. 3e). Consequently, the WMS U/Th ratio appears to be predominantly sensitive to suboxic conditions at the sea floor, and furthermore correlates with organic matter deposition.

4. Results

Major element concentrations in 355 samples were obtained by AAS; 360 samples were analyzed using inductively coupled plasma-mass spectrometry. Nd isotopic composition was determined in 15 samples, 11 in the authigenic Fe-Mn oxide coatings around foraminifera tests and 4 in bulk samples (Table 2). All datasets are unpublished to date, except the Barium excess content during the 20 to 5 kyr interval, previously discussed in Jimenez-Espejo et al. (2008).

U content ranged between 1 and 5 ppm, showing the lowest values at site 304G during late Holocene. Higher values are associated to the deglaciation period (U > 3 ppm), whereas lower values can be found during the last Glacial maximum and after 8.0 kyr. The content varies between 5 and 9 ppm, the highest values reached during late Holocene at site 302G.

The Ba content derived from marine barite (Ba excess) was obtained by subtracting the amount of terrigenous Ba from the total Ba content (Dymond et al., 1992; Eagle et al., 2003). The presence of marine barite was confirmed by Field Emission Scanning Electron Microscopy (FESEM). Barite crystals were found with sizes and morphologies corresponding to typical marine barite (1–5 mm in size, with round and elliptical crystals). Ba excess is calculated as: Ba excess = (Ba-total) − Al $(Ba/Al)_c$, where Ba-total and Al are concentrations in ppm, and $(Ba/Al)_c$ is the crustal ratio for these elements. In this study, we used the value $(Ba/Al)_c = 0.033$, as estimated by Sanchez-Vidal et al. (2005) in the Alboran basin. During the last 5 ka interval all studied sites show a nearly parallel and flat pattern, having Ba excess values around 250 ppm (Fig. 3e).

In turn, the ε_{Nd} values obtained for the authigenic fraction range from $\varepsilon_{Nd} - 10.1 \pm 0.3$ for the deepest site (304G) during the last glacial period, to $\varepsilon_{Nd} - 9.09 \pm 0.28$ for the shallowest site (302G) during late Holocene. Measured ε_{Nd} values in bulk samples are clearly different from the authigenic ones, with ε_{Nd} values between -12.62 ± 0.28 and -12.82 ± 0.28 (Table 2).

5. Discussion

5.1. Last Glacial Maximum and deglaciation

During the last glacial maximum, a low sea level combined with cold and arid conditions over the Gulf of Lion (Hayes et al., 2005) have been associated with intense deep water formation in the WMS (Rogerson et al., 2008). Around 19.8 ka cal BP we obtained a ε_{Nd} value of -9.6 ± 0.29 for site 302G and $\varepsilon_{Nd} - 10.1 \pm 0.3$ for site 304G (Fig. 3b), values typically associated with modern water masses generated in the Gulf of Lion (Henry et al., 1994; Tachikawa et al., 2004) (Fig. 3b). At all our studied sites U/Th ratios show relatively low values, between 0.25 and 0.4, suggesting well ventilated water mass generated in the WMS. For the same time period, Toucanne et al. (2012) described an intense LIW flow at the Corsica Trough (MD01-2434; Fig. 3d). Furthermore, a dense MOW, flowing at deeper depths than today, has been reconstructed in the Gulf of Cadiz (Rogerson et al., 2005; Voelker et al., 2006; Llave et al., 2007), with low activity in the upper MOW branch (Bahr et al., 2014). We therefore conclude that WMDW predominance in the Alboran basin is coincident with enhanced activity of the

deeper MOW branch during the last glacial maximum. The probable causes of this relationship will be discussed in more detail below.

Environmental conditions in the Alboran Sea appear to change around 18 ka cal BP, contemporaneous with progressive deglaciation affecting atmospheric CO_2 and methane contents (e.g., Marcott et al., 2014), as well as the Atlantic meridional circulation (McManus et al., 2004). Our Nd records indicate a shift from values around -10.1 ± 0.3 during the glacial period, to less radiogenic ones reaching $\varepsilon_{Nd} = -9.0 \pm 0.3$ at site 302G at 15.8 ka cal BP (Fig. 3b). Such higher values are typically associated with water masses generated in the EMS (Henry et al., 1994; Tachikawa et al., 2004). Furthermore, from 17.5 ka cal BP onward U/Th ratios increase at all sites, with a subtle difference among them (Fig. 3 dashed line). At the shallower sites, 300G and 302G, oxygenation decreases before the same trend is observed at the deeper site 304G, pointing to a depth-dependent bottom and/or pore waters ventilation. Despite the dating uncertainties, similar depth-dependent ventilation variations have been invoked in the EMS basins related to sapropel S1 deposition (De Lange et al., 2008; Tachikawa et al., 2015). These changes can be explained by progressive water mass mixing or replacement of WMS-generated deep waters, and/or by deepening of EMS-generated intermediate waters (LIW) from 1900 and 2300 mbsf. It is noteworthy that we observe a peak in LIW intensity in the Corsica site (Toucanne et al., 2012: Fig. 3d) at the same time when the mLIW influence appears to affect the shallowest sites in the Alboran Sea. This decrease in the WMDW contribution to the MOW should have increased the MOW buoyancy and decreased the flux in the lower core of the MOW, as can be interpreted from the records in the Gulf of Cadiz (Voelker et al., 2006). Nevertheless, no changes are observed in the MOW upper branch (Fig. 3c) (Bahr et al., 2014). Hence, changes in water masses within the Alboran region can be tracked in the Gulf of Cadiz, in this case a mLIW intensification that is connected to a ceased MOW lower core.

The next change in environmental conditions that is recorded in the Alboran region took place during the GS-1 (Younger Dryas, YD) (Fig. 3). Ba/Al and U/Th ratios show an increase during the YD at the deepest site (304G), pointing to lower oxygenation and higher productivity, which coincides with the maximum intensity of LIW flow in the central Mediterranean Sea (Fig. 3d) (Toucanne et al., 2012). This increase in marine productivity is also documented by the diatom record from Alboran basin (Barcena et al., 2001). In the Gulf of Cadiz (Site U1387; Bahr et al., 2014), a concomitant reactivation of the upper branch of MOW, as reconstructed from Zr/Al ratios, indicates higher MOW buoyancy during this period (Fig. 3c). A weak contribution of the WMDW to the MOW is fostered by the Nd data that point to a persistent influence of the LIW waters at site 302G (Fig. 3b). Furthermore, the studied proxies indicate that the cooling associated with the YD did not lead to a significant reactivation of WMDW formation. This observed low oxygenation in the WMS during the YD seems to contradict model results that predict high ventilation during this period (Rogerson et al., 2012a). Our data therefore reveal a marked difference between the EMS, with intense thermohaline circulation, and the WMS, with sluggish circulation during the YD. It appears that the Eastern Mediterranean Basin was more prone to alterations in the water mass structure than the western basin (Sprovieri et al., 2012; Hayes et al., 2005; Hennekam et al., 2014).

5.2. Holocene and sapropel deposition

During the Holocene, the Eastern and Western Mediterranean Basins show distinct signatures. In the Eastern basin, a characteristic feature was the deposition of the most recent sapropel (S1), an organic-rich black layer, deposited between 10.8 ± 0.4 and 6.1 ± 0.5 ka cal BP (Ariztegui et al., 2000; De Lange et al., 2008). However, no such deposits can be found in the WMS, where the last ORL formed between 14.5 and 8.2 ka (Cacho et al., 2002; Rogerson et al., 2008; Rohling et al., 2015).

During the early/middle Holocene (until 8.2 ka BP), the studied records display high U/Th ratio values (around 0.6), indicating a relatively low oxygenation in agreement with the S1a deposition (Fig. 3a). The Nd isotopic composition of seawater around 6.8 ka cal BP at site 302G ($\varepsilon_{Nd} - 9.75 \pm 0.27$) shows values similar to those related with WMDW formation during the Last Glacial Maximum, pointing to a WMDW reactivation — or at least a LIW reduction — while sapropel S1 deposition was still active. Weak LIW formation has also been described in the EMS during sapropel deposition and has been linked with increase runoff and fluvial input from the Nile (Bosmans et al., 2015a,b; Rohling et al., 2015).

During the late Holocene, more radiogenic Nd isotope values indicate a mLIW influence (Fig. 3b). This recovery of the EMS signal is coincident with a progressive increase in the MOW upper branch (Fig. 3c). Notably, the central Mediterranean LIW record (Fig. 3d) does not show any variations associated with the sapropel demise, nor does it reveal any significant changes throughout the entire Holocene. Previous work has described an antiphased pattern between the EMS and the WMS in the late Holocene (Rimbu et al., 2004; Roberts et al., 2008; Felis and Rimbu, 2010; Martín-Puertas et al., 2010), with humid conditions in the WMS (Martín-Puertas et al., 2010) but dry conditions in the EMS (e.g., Nieto-Moreno et al., 2013). These differences between basins can be related to the W-E gradients in salinity and temperature, different influences of riverine input, and diverging climate patterns especially during winter (e.g., Hayes et al., 2005).

Overall, observed variations during the Holocene indicate a high sensitivity of the Mediterranean thermohaline circulation to fresh water input. In detail, model results indicate that as little as 5%-10% changes in the Mediterranean mean freshwater budget may have pronounced effects on the overturning circulation in the area (Skliris et al., 2007).

5.3. Origin and significance of simultaneous changes recorded between records from the Alboran Sea and MOW

Comparison between our records from the Alboran sites and previously published MOW records indicates a complex regional picture. Despite the fact that the WMS thermohaline circulation is affected by a number of factors throughout time — such as interaction between sea-level rise, meltwater pulses, monsoon flooding, Gibraltar strait section and Alpine melt-water routing (e.g., Rohling et al., 2015) — our new data reveal some insightful patterns. In detail, our observations indicate that (i) the MOW's lower branch is linked to the WMDW evolution, (ii) its middle branch follows the LIW activity, and (iii) its upper branch is more active during times of minima in WMDW formation. This marked heterogeneity of the MOW is in agreement with present day oceanographic observations of different Mediterranean waters in the Gibraltar strait (Naranjo et al., 2012; Millot, 2014) and three distinct MOW branches (e.g., Ambar et al., 2002).

The described correlations between the two water masses can be causal or genetic. A causal relation would have major consequences for understanding the MOW behavior, because the WMDW, formed in the Gulf of Lion, is mainly driven by the North Atlantic climate realm (Cacho et al., 2002; Frigola et al., 2007). In contrast, the LIW is mainly affected by the Eastern Mediterranean realm and conditioned by variations in high and low latitude climates (e.g., Blanchet et al., 2013; Hennekam et al., 2014). If causal, the main mechanisms driving the MOW branch intensification could be freshening of the Mediterranean Sea surface, thereby influencing bottom water formation (MerMex Group et al., 2011). Enhanced fresh water input has been related to Nile run-off (Rossignol-Strick et al., 1982; Rohling, 1994; Rohling et al., 2015), meltwater fluxes (Ehrmann et al., 2007), and Black Sea influence (Grimm et al., 2015). Climate models indicate that precipitation patterns as well as runoff from the Nile are driven by the strength of the North African monsoon, ultimately responding to northern hemisphere summer insolation (Bosmans et al., 2015a,b). In such a scenario, water mass variations at the studied core sites can be interpreted to manifest

the influence of surface processes on deep sea circulation in the Mediterranean.

Nonetheless, hydrodynamic models reject a causal link between downwelling in the Mediterranean and MOW evolution, and instead propose sea-level variability and water column density in the Eastern Atlantic as main driving factors for MOW deepening and branch activity (Rogerson et al., 2012a,b). In this case, the described correlation between both sides of the Gibraltar strait water masses could be linked genetically, through common climate and environmental variations. More specifically, the water column density gradient in the Gulf of Cadiz would have increased during deglaciation due to the production of meltwater from ice sheets and glaciers (Rogerson et al., 2012b). This gradient increase would in turn promote a MOW shoaling due to the presence of dense Atlantic water masses at shallower depths and surface freshening in the Mediterranean, leading to reduced WMDW formation at the same time. This genetic link is, however, difficult to reconcile with observed changes during the late Holocene, a period of almost stable sea level.

No matter which of the two mechanisms is preferred, our data certainly point to an intrinsic correlation between Mediterranean intermediate water masses and MOW branches. Deciphering this correlation in more detail calls for a targeted study of geochemical proxies in all three MOW branches (lower, middle, and upper) to discern whether they preserve an EMS or WMS climate realm signal. Based on the results presented here, we can speculate that the middle and upper branch were probably dominated by low latitude climate variations, whereas the lower branch would be more sensitive to a higher latitudinal signal.

6. Conclusions

Geochemical proxies provide evidence of significant paleoceanographic changes in the western Mediterranean during the last 20 ka BP. We observe a replacement (or reduced influence) of relatively cold and well oxygenated bottom waters generated in the WMS during GS-2a by less oxygenated intermediate water masses of Eastern Mediterranean provenance in key depth locations. The Eastern water mass appears to have influenced shallower water depths in the Alboran Sea during the entire deglaciation and until the early Holocene.

Comparison of the Alboran records with previously published records of LIW intensity from the Central Mediterranean, as well as MOW intensity in the Gulf of Cadiz, suggests a heterogeneous MOW linked to Mediterranean intermediate water variations. The lower branch seems to be mainly fed by the WMDW, while the middle and upper branch would be linked to LIW activity. Nevertheless, we cannot determine whether the described relationships are causally or genetically based. Placing our results into the context of Northern Hemisphere climate variations, the lower branch of MOW is apparently dominated by high latitude climate variations, and the middle and upper branches are instead forced by low latitude evolution. More detailed studies are needed to fully resolve what drives changes in the different branches of MOW over time, and how they are associated with regional and global climate changes.

Acknowledgements

The authors are indebted to Dr. Zhengtang Guo as editor, Dr. M. Rogerson and two anonymous reviewers for their invaluable comments and reviews. This study was supported by the European Regional Development Fund (ERDF)-financed grants CGL2009-07603 and CGL2012-32659 (Secretaría de Estado de Investigación MINECO), Project RNM 5212 and Research Group RNM 179 (Junta de Andalucía). We are grateful to the Training-Through-Research Programme for providing the core sediments analyzed. We acknowledge the Centre for Scientific Instrumentation (CIC—University of Granada), the Poznan Radiocarbon Laboratory (Poland), Andalusian Institute of Earth Sciences (IACT, CSIC-UGR), Department of Mineralogy and Petrology (UGR) and Imperial College (U.K.) for analytical facilities. We also thank D. Ortega and E. Holanda, C. Niembro, L. González, E. Abarca and J. Santamarina, as well as the CIC personnel for their laboratory assistance. T.T. measurements are supported by grants-in-aid for scientific research by MEXT/JSPS (2074031 and 25247085 to T.T.).

Appendix A. Supplementary data

Supplementary data to this article can be found online at http://dx.doi.org/10.1016/j.gloplacha.2015.10.001.

References

Ambar, I., Serra, A., Brogueira, M.J., Cabeçadas, G., Abrantes, F., Freitas, P., Gonçalves, C., Gonzalez, N., 2002. Physical, chemical and sedimentological aspects of the Mediterranean outflow off Iberia. Deep-Sea Res. II Top. Stud. Oceanogr. 49, 4163–4177.

Andersen, M.B., Romaniello, S., Vance, V., Little, S.H., Herdman, R., Lyons, T.W., 2014. A modern framework for the interpretation of 238 U/235 U in studies of ancient ocean redox. Earth Planet. Sci. Lett. 400, 184–194.

Anderson, R.F., 1982. Concentration, vertical flux and remineralization of particulate uranium in seawater. Geochim. Cosmochim. Acta 46, 1293–1299.

Ariztegui, A., Asioli, J.J., Lowe, F., Trincardi, L., Vigliotti, F., Tamburini, C., Chondrogianni, C.A., Accorsi, M., Bandini Mazzanti, A.M., Mercuri, S., Van der Kaars, J.A., McKenzie, J., 2000. Palaeoclimate and the formation of sapropel S1: inferences from Late Quaternary lacustrine and marine sequences in the central Mediterranean region. Palaeogeogr. Palaeoclimatol. Palaeoecol. 158 (3), 215–240. http://dx.doi.org/10.1016/S0031-0182(00)00051-1.

Bahr, A., Jiménez-Espejo, F.J., Kolasinac, N., Grunert, P., Hernandéz-Molina, F.J., Röhl, U., Voelker, A.H.L., Escutia, C., Stow, D.A.V., Alvarez-Zarikian, C.A., Hodell, D.A., 2014. Deciphering bottom current strength and paleoclimate signals from contourite deposits in the gulf of Cádiz during the last 140 ka: an inorganic geochemical approach. Geochem. Geophys. Geosyst. 15 (8), 3145–3160. http://dx.doi.org/10.1002/2014GC005356.

Barcena, M.A., Cacho, I., Abrantes, F., Sierro, F.J., Grimalt, J.O., Flores, J.A., 2001. Paleoproductivity variations related to climatic conditions in the Alboran Sea (western Mediterranean) during the last glacial–interglacial transition: the diatom record. Palaeogeogr. Palaeoclimatol. Palaeoecol. 167, 337–357.

Barnes, C.E., Cochran, J.K., 1990. Uranium removal in oceanic sediments and the oceanic U balance. Earth Planet. Sci. Lett. 97, 94–101.

Bea, F., 1996. Residence of REE, Y, Th and U in granites and crustal protoliths; implications for the chemistry of crustal melts. J. Petrol. 37, 521–552. http://dx.doi.org/10.1093/petrology/ 37.3.521.

Bethoux, J.P., Morin, P., Chaumery, C., Connan, O., Gentili, B., Ruiz Pino, D., 1998. Nutrients in the Mediterranean Sea, mass balance and statistical analysis of concentrations with respect to environmental change. Mar. Chem. 63, 155–169. http://dx.doi.org/10.1016/S0304-4203(98)00059-0.

Biscaye, P.E., 1965. Mineralogy and sedimentation of recent deep-sea clay in the Atlantic Ocean and adjacent seas and oceans. Geol. Soc. Am. Bull. 76, 803–831.

Blanchet, C.L., Tjallingii, R., Frank, M., Lorenzen, J., Reitz, A., Brown, K., Feseker, T., Brückmann, W., 2013. High- and low-latitude forcing of the Nile River regime during the Holocene inferred from laminated sediments of the Nile deep-sea fan. Earth Planet. Sci. Lett. 364, 98–110.

Bosmans, J.H.C., Drijfhout, S.S., Tuenter, E., Hilgen, F.J., Lourens, L.J., 2015a. Response of the North African summer monsoon to precession and obliquity forcings in the EC-Earth GCM. Clim. Dyn. 44, 279–297.

Bosmans, J.H.C., Drijfhout, S., Tuenter, E., Hilgen, F.J., Lourens, L.J., Rohling, E.J., 2015b. Precession and obliquity forcing of the freshwater budget over the Mediterranean. Quat. Sci. Rev. 123, 16–30.

Bryden, H.L., Stommel, H.M., 1984. Limiting processes that determine basic features of the circulation in the Mediterranean Sea. Oceanol. Acta 7, 289–296.

Cacho, I., Grimalt, J.O., Canals, M., Sbaffi, L., Shackleton, N., Schonfeld, J., Zahn, R., 2001. Variability of the western Mediterranean Sea surface temperature during the last 25 000 years and its connection with the northern hemisphere climatic changes. Paleoceanography 16, 40–52.

Cacho, I., Sierro, F., Shackleton, N.J., Elderfield, H., Grimalt, J., 2002. Reconstructing Alboran Sea hydrography during the last organic rich layer formation. Geochim. Cosmochim. Acta 66 (A115).

Calvert, S.E., Pedersen, T.F., 2007. Elemental proxies for palaeoclimatic and palaeoceanographic variability in marine sediments: interpretation and application. In: Hillaire-Marcel, C., Vernal, A.D. (Eds.), Proxies in Late Cenozoic Paleoceanography. Elsevier, Amsterdam.

Chase, Z., Anderson, R.F., Fleisher, M.Q., 2001. Evidence from authigenic uranium for increased productivity of the glacial subantarctic ocean. Paleoceanography 16, 468–478.

Comas, M.C., Ivanov, M.K., 2006. Eastern Alboran margin: the transition between the Alboran and the Balearic–Algerian basins. In: Kenyon, H., Ivanov, M.K., Akhmetzhanov, A.M., Kozlova, E.V. (Eds.), Interdisciplinary Geoscience Studies of the Gulf of Cadiz and Western Mediterranean BasinsIOC Technical Series. UNESCO, pp. 48–55.

Cramp, A., O'Sullivan, G., 1999. Neogene sapropels in the Mediterranean: a review. Mar. Geol. 153, 11–28. http://dx.doi.org/10.1016/S0025-3227(98)00092-9.

De Lange, G.J., Thomson, J., Reitz, A., Slomp, C.P., Principato, M.S., Erba, E., Corselli, C., 2008. Synchronous basin-wide formation and redoc-controlled preservation of a Mediterranean sapropel. Nat. Geosci. 1, 606–610.

Dymond, J., Suess, E., Lyle, J.M., 1992. Barium in deepsea sediment: a geochemical proxy for paleoproductivity. Paleoceanography 7, 163–181. http://dx.doi.org/10.1029/92PA00181.

Eagle, M., Paytan, A., Arrigo, K., Van Dijken, G., Murray, R., 2003. A comparison between excess barium and barite as indicators of export production. Paleoceanography 18, 1021. http://dx.doi.org/10.1029/2002PA000793.

Ehrmann, W.U., Schmiedl, G., Hamann, Y., Kuhnt, T., Hemleben, C., Siebel, W., 2007. Clay minerals in late glacial and Holocene sediments of the northern and southern Aegean Sea. Palaeogeogr. Palaeoclimatol. Palaeoecol. 249 (1–2), 36–57. http://dx.doi.org/10.1016/j.palaeo.2007.01.004.

Felis, T., Rimbu, N., 2010. Mediterranean climate variability documented in oxygen isotope records from northern Red Sea corals. A review. Glob. Planet. Chang. 71, 232–241.

Font, J., 1987. The path of the Levantine intermediate water to the Alboran Sea. Deep-Sea Res. 34, 1745–1755.

Frank, M., Whiteley, N., Kasten, S., Hein, J.R., O'Nions, R.K., 2002. North Atlantic deep water export to the southern ocean over the past 14 Myr: evidence from Nd and Pb isotopes in ferromanganese crusts. Paleoceanography 17, 1022. http://dx.doi.org/10.1029/2000PA000606.

Frigola, J., Moreno, A., Cacho, I., Canals, M., Sierro, F.J., Flores, J.A., Grimalt, J.O., Hodell, D.A., Curtis, J.H., 2007. Holocene climate variability in the western Mediterranean region from a deepwater sediment record. Paleoceanography 22, PA2209. http://dx.doi.org/10.1029/2006PA001307.

Goldstein, S.L., Hemming, S.R., 2003. Long-lived isotopic tracers in oceanography, paleoceanography and ice sheet dynamics. In: Elderfield, H. (Ed.), Treatise on Geochemistry. Elsevier, Oxford, pp. 453–489.

Grimm, R., Maier-Reimer, E., Mikolajewicz, U., Schmiedl, G., Müller-Navarra, K., Adloff, F., Grant, K.M., Ziegler, M., Lourens, L.J., Emeis, K.-C., 2015. Late glacial initiation of Holocene eastern Mediterranean sapropel formation. Nat. Geosci. 6, 7099. http://dx.doi.org/10.1038/ncomms8099.

Gutjahr, M., Frank, M., Stirling, C.H., Keigwin, L.D., Halliday, A.N., 2008. Tracing the Nd isotope evolution of north Atlantic deep and intermediate waters in the western north Atlantic since the Last Glacial Maximum from Blake Ridge sediments. Earth Planet. Sci. Lett. 266, 61–77.

Hayes, A., Kucera, M., Kallel, N., Sbeffi, L., Rohling, E.J., 2005. Glacial Mediterranean Sea surface temperatures based on planktonic foraminiferal assemblages. Quat. Sci. Rev. 24, 999–1016.

Hennekam, R., Jilbert, T., Schnetger, B., de Lange, G.J., 2014. Solar forcing of Nile discharge and sapropel S1 formation in the early to middle Holocene eastern Mediterranean. Paleoceanography 29 (2013PA002553).

Henry, F., Jeandel, C., Minster, J.F., 1994. Particulate and dissolved Nd in the Western Mediterranean Sea: sources, fates and budget. Mar. Chem. 45, 283–305.

Hernandez-Molina, F.J., Somoza, L., Vázquez, J.T., Lobo, F., Fernández-Puga, M.C., Llave, E., Díaz del Río, V., 2002. Quaternary stratigraphic stacking patterns on the continental shelves of the southern Iberian Peninsula: their relationship with global climate and paleoceanographic changes. Quat. Int. 92, 5–23.

Hernandez-Molina, F.J., Stow, D.A.V., Alvarez-Zarikian, C.A., Acton, G., Bahr, A., Balestra, B., Ducassou, E., Flood, R., Flores, J.-A., Furota, S., Grunert, P., Hodell, D., Jimenez-Espejo, F.J., Kim, J.K., Krissek, L., Kuroda, J., Li, B., Llave, E., Lofi, J., Lourens, L., Miller, M., Nanayama, F., Nishida, N., Richter, C., Roque, C., Pereira, H., Sanchez-Goñi, M.F., Sierro, F.J., Singh, A.D., Sloss, C., Takashimizu, Y., Tzanova, A., Voelker, A., Williams, T., Xuan, C., 2014. Onset of Mediterranean outflow into the North Atlantic. Science 344, 1244–1250. http://dx.doi.org/10.1126/science.1251306.

Ivanovic, R.F., Valdes, P.J., Gregoire, L., Flecker, R., Gutjahr, M., 2014. Sensitivity of modern climate to the presence, strength and salinity of Mediterranean–Atlantic exchange in a global general circulation model. Clim. Dyn. 42, 859–877. http://dx.doi.org/10.1007/s00382-013-1680-5.

Jacobsen, S.B., Wasserburg, G.J., 1980. Sm/Nd isotopic evolution of chondrites. Earth Planet. Sci. Lett. 50, 139–155.

Jeandel, C., Aesouze, T., Lacan, F., Téchiné, P., Dutay, J.-C., 2007. Isotopic Nd compositions and concentrations of the lithogenic inputs into the ocean: a compilation, with an emphasis on the margins. Chem. Geol. 239, 156–164.

Jimenez-Espejo, F.J., Martinez-Ruiz, F., Sakamoto, T., Iijima, K., Gallego-Torres, D., Harada, N., 2007. Paleoenvironmental changes in the western Mediterranean since the last glacial maximum: high resolution multiproxy record from the Algero–Balearic basin. Palaeogeogr. Palaeoclimatol. Palaeoecol. 246, 292–306.

Jimenez-Espejo, F.J., Martinez-Ruiz, M., Rogerson, M., Gonzalez-Donoso, J.M., Romero, O.E., Linares, D., Sakamoto, T., Gallego-Torres, D., Rueda-Ruiz, J.L., Ortega-Huertas, M., Perez-Claros, J.A., 2008. Detrital input, productivity fluctuations, and water mass circulation in the westernmost Mediterranean Sea since the Last Glacial Maximum. Geochem. Geophys. Geosyst. 9, Q11U02. http://dx.doi.org/10.1029/2008GC002096.

Johnson, R.G., 1997. Climate control requires a dam at the Strait of Gibraltar. Eos Trans. AGU 78 (277), 280–281.

Lacan, F., Tachikawa, K., Jeandel, C., 2012. Neodymium isotopic composition of the oceans: a compilation of seawater data. Chem. Geol. 300-301, 177–194.

Llave, E., Hernández-Molina, F.J., Somoza, L., Stow, D.A.V., Díaz Del Río, V., 2007. Quaternary evolution of the contourite depositional system in the Gulf of Cádiz. Geol. Soc. Spec. Publ. 276, 49–79. http://dx.doi.org/10.1144/GSL.SP.2007.276.01.03.

Mangini, A., Jung, M., Laukenmann, S., 2001. What do we learn from peaks of uranium and of manganese in deep sea sediments? Mar. Geol. 177, 63–78.

Marcott, S.A., Bauska, T.K., Buizert, C., Steig, E.J., Rosen, J.L., Cuffey, K.M., Fudge, T.J., Severinghaus, J.P., Ahn, J., Kalk, M.L., McConnell, J.R., Sowers, T., Taylor, K.C., White, J.W.C., Brook, E.J., 2014. Centennial-scale changes in the global carbon cycle during the last deglaciation. Nature 514, 616–619.

Martín-Puertas, C., Jiménez-Espejo, F.J., Martinez-Ruiz, F., Nieto-Moreno, V., Rodrigo, M., Mata, M.P., Valero-Garcés, B.L., 2010. Late Holocene climate variability in the southwestern Mediterranean region: an integrated marine and terrestrial geochemical approach. Clim. Past 6, 807–816.

Martrat, B., Grimalt, J.O., Lopez-Martinez, C., Cacho, I., Sierro, F.J., Flores, J.A., Zahn, R., Canals, M., Curtis, J.H., Hodell, D.A., 2004. Abrupt temperature changes in the western Mediterranean over the past 250,000 years. Science 306, 1762–1765.

McManus, J.F., Francois, R., Gherardi, J.-M., Keigwin, L.D., Brown-Leger, S., 2004. Collapse and rapid resumption of Atlantic meridional circulation linked to deglacial climate changes. Nature 428, 834–837. http://dx.doi.org/10.1038/nature02494.

MerMex Group, Durrieu de Madron, X., Guieu, C., Sempéré, R., Conan, P., Cossa, D., D'Ortenzio, F., Estournel, C., Gazeau, F., Rabouille, C., Stemmann, L., Bonnet, S., Diaz, F., Koubbi, P., Radakovitch, O., Babin, M., Baklouti, M., Bancon-Montigny, C., Belviso, S., Bensoussan, N., Bonsang, B., Bouloubassi, I., Brunet, C., Cadiou, J.-F., Carlotti, F., Chami, M., Charmasson, S., Charrière, B., Dachs, J., Doxaran, D., Dutay, J.-C., Elbaz-Poulichet, F., 2011. Marine ecosystems' responses to climatic and anthropogenic forcings in the Mediterranean. Prog. Oceanogr. 91, 97–166.

Millot, C.J., 1999. Circulation in the western Mediterranean Sea. J. Mar. Syst. 20, 423–442. http://dx.doi.org/10.1016/S0924-7963(98).00078-5.

Millot, C.J., 2009. Another description of the Mediterranean Sea outflow. Prog. Oceanogr. 82, 101–124. http://dx.doi.org/10.1016/j. pocean.2009.04.016.

Millot, C.J., 2014. Heterogeneities of in-and out-flows in the Mediterranean Sea. Prog. Oceanogr. 120, 254–278. http://dx.doi.org/10.1016/ j.pocean.2013.09.007.

Moreno, A., Cacho, I., Canals, M., Grimalt, J.O., Sanchez-Goñi, M.F., Shackleton, N., Sierro, F.J., 2005. Links between marine and atmospheric processes oscillating on a millennial time-scale. A multi-proxy study of the last 50,000 yr from the Alboran Sea (Western Mediterranean Sea). Quat. Sci. Rev. 24, 1623–1636.

Naranjo, C., García-Lafuente, J., Sánchez-Garrido, J.C., Sánchez-Román, A., Delgado-Cabello, J., 2012. The Western Alboran Gyre helps ventilate the Western Mediterranean deep water through Gibraltar. Deep-Sea Res. I 63, 157–163. http://dx.doi.org/10.1016/j.dsr.2011.10.003.

Nieto-Moreno, V., Martinez-Ruiz, F., Willmott, V., García-Orellana, J., Masque, P., Sinninghe-Damste, J.S., 2013. Climate conditions in the westernmost Mediterranean over the last two millennia: an integrated biomarker approach. Org. Geochem. 55, 1–10. http://dx.doi.org/10.1016/j.orggeochem.2012.11.001.

Ovchinnikov, I.M., Plakhin, A., Moskalenko, L.V., Neglyad, K.V., Osadchiy, A.S., Fedoseyev, A.F., Krivoscheya, V.G., Voytova, K.V., 1976. Hydrology of the Mediterranean Sea. Gidrometeoizdat, Leningrad (375 pp.).

Palomino, D., Vázquez, J.-T., Ercilla, G., Alonso, B., López-González, N., Díaz-del-Río, V., 2011. Interaction between seabed morphology and water masses around the seamounts on the Motril Marginal Plateau (Alboran Sea, Western Mediterranean). Geo-Mar. Lett. 31, 465–479.

Parrilla, G., Kinder, T.H., Preller, R.H., 1986. Deep and intermediate Mediterranean water in the western Alboran Sea. Deep-Sea Res. I 33, 55–88.

Pin, C., Zalduegui, J.S., 1997. Sequential separation of light rare-earth elements, thorium and uranium by miniaturized extraction chromatography: application to isotopic analyses of silicate rocks. Anal. Chim. Acta 339, 79–89.

Rimbu, N., Lohmann, G., Lorenz, S.J., Kim, J.H., Schneider, R.R., 2004. Holocene climate variability as derived from alkenone sea surface temperature and coupled ocean–atmosphere model experiments. Clim. Dyn. 23, 215–227. http://dx.doi.org/10.1007/s00382-004-0435-8.

Roberts, N., Jones, M.D., Benkaddour, A., Eastwood, W.J., Filippi, M.L., Frogley, M.R., Lamb, H.F., Leng, M.J., Reed, J.M., Stein, M., Stevens, L., Valero-Garcés, B., Zanchetta, G., 2008. Stable isotope records of late quaternary climate and hydrology from Mediterranean lakes: the ISOMED synthesis. Quat. Sci. Rev. 27 (25–26), 2426–2441. http://dx.doi.org/10.1016/ j.quascirev.2008.09.005.

Roberts, N.L., Piotrowski, A.M., McManus, J.F., Keigwin, L.D., 2010. Synchronous deglacial overturning and water mass source changes. Science 327, 75–78.

Rogerson, M., Rohling, E.J., Weaver, P.P.E., Murray, J.W., 2005. Glacial to interglacial changes in the settling depth of the Mediterranean Outflow plume. Paleoceanography 20, PA3007. http://dx.doi.org/10.1029/2004PA001106.

Rogerson, M., Rohling, E.J., Weaver, P.P.E., 2006. Promotion of meridional overturning by Mediterranean-derived salt during the last deglaciation. Paleoceanography 21, PA4101. http://dx.doi.org/10.1029/2006PA001306.

Rogerson, M., Cacho, I., Jimenez-Espejo, F.J., Reguera, M.I., Sierro, F.J., Martinez-Ruiz, F., Frigola, J., Canals, M., 2008. A dynamic explanation for the origin of the western Mediterranean organic-rich layers. Geochem. Geophys. Geosyst. 9, Q07U01. http://dx.doi.org/10.1029/2007GC001936.

Rogerson, M., Bigg, G.R., Rohling, E.J., Ramirez, J., 2012a. Vertical density gradient in the eastern North Atlantic during the last 30,000 years. Clim. Dyn. 39, 589–598.

Rogerson, M., Rohling, E.J., Bigg, G.R., Ramirez, J., 2012b. Paleoceanography of the Atlantic-Mediterranean exchange: overview and first quantitative assessment of climatic forcing. Rev. Geophys. 50, RG2003. http://dx.doi.org/10.1029/2011rg000376.

Rohling, E.J., 1994. Review and new aspects concerning the formation of Mediterranean sapropels. Mar. Geol. 122, 1–28.

Rohling, E.J., Bryden, H.L., 1992. Man-induced salinity and temperature increases in western Mediterranean deep water. J. Geophys. Res. 97. http://dx.doi.org/10.1029/92JC00767.

Rohling, E.J., Marino, G., Grant, K.M., 2015. Mediterranean climate and oceanography, and the periodic development of anoxic events (sapropels). Earth Sci. Rev. 143, 62–97. http://dx.doi.org/10.1016/j.earscirev.2015.01.008.

Rossignol-Strick, M., Nesteroff, W., Olive, P., Vergnaud-Grazzini, C., 1982. After the deluge: Mediterranean stagnation and sapropel formation. Nature 295, 105–110.

Rutberg, R.L., Hemming, S.R., Goldstein, S.L., 2000. Reduced North Atlantic deep water flux to the glacial southern ocean inferred from neodymium isotope ratios. Nature 405, 935–938.

Sanchez-Vidal, A., Collier, R.W., Calafat, A., Fabres, J., Canals, M., 2005. Particulate barium fluxes on the continental margin: a study from the alboran sea (western Mediterranean). Mar. Chem. 93, 105–117. http://dx.doi.org/10.1016/j.marchem.2004.07.004.

Sierro, F.J., Hodell, D.A., Curtis, J.H., Flores, J.A., Reguera, I., Colmenero-Hidalgo, E., Bárcena, M.A., Grimalt, J.O., Cacho, I., Frigola, J., Canals, M., 2005. Impact of iceberg melting on Mediterranean thermohaline circulation during Heinrich events. Paleoceanography 20, PA2019. http://dx.doi.org/10.1029/2004PA001051.

Skliris, N., Sofianos, S., Lascaratos, A., 2007. Hydrological changes in the Mediterranean sea in relation to changes in the freshwater budget: a numerical modelling study. J. Mar. Syst. 65, 400–416. http://dx.doi.org/10.1016/j.jmarsys.2006.01.015.

Spivack, A.J., Wasserburg, G.J., 1988. Neodymium isotopic composition of the Mediterranean outflow and the eastern North Atlantic. Geochim. Cosmochim. Acta 52, 2762–2773.

Sprovieri, M., Di Stefano, E., Incarbona, A., Salvagio Manta, D., Pelosi, N., Ribera d'Alcala, M., Sprovieri, R., 2012. Centennial- to millennial-scale climate oscillations in the Central–Eastern Mediterranean Sea between 20,000 and 70,000 years ago: evidence from a high-resolution geochemical and micropaleontological record. Quat. Sci. Rev. 46, 126–135. http://dx.doi.org/10.1016/j.quascirev.2012.05.005.

Stumpf, R., Frank, M., Schönfeld, J., Haley, B.A., 2010. Late Quaternary variability of Mediterranean Outflow Water from radiogenic Nd and Pb isotopes. Quat. Sci. Rev. 29 (19–20), 2462–2472. http://dx.doi.org/10.1016/j.quascirev.2010.06.021.

Tachikawa, K., Athias, V., Jeandel, C., 2003. Neodymium budget in the modern ocean and paleoceanographic implications. J. Geophys. Res. Oceans (1978–2012) 108, 3254. http://dx.doi.org/10.1029/1999JC000285.

Tachikawa, K., Roy-Barman, M., Michard, A., Thouron, D., Yeghicheyan, D., Jeandel, C., 2004. Neodymium isotopes in the Mediterranean sea: comparison between seawater and sediment signals. Geochim. Cosmochim. Acta 68 (14), 3095–3106.

Tachikawa, K., Vidal, L., Cornuault, M., Garcial, M., Pothin, A., Sonzogni, C., Bard, E., Menot, G., Revel, M., 2015. Eastern Mediterranean sea circulation inferred from the conditions of S1 sapropel deposition. Clim. Past 11, 855–867. http://dx.doi.org/10.5194/cp-11-855-2015.

Tanaka, T., Togashi, S., Kamioka, H., Amakawa, H., Kagami, H., Hamamoto, T., Yuhara, M., Orihashi, Y., Yoneda, S., Shimizu, H., Kunimaru, T., Takahashi, K., Yanagi, T., Nakano, T., Fujimaki, H., Shinjo, R., Asahara, Y., Tanimizu, M., Dragusanu, C., 2000. JNdi-1: a neodymium isotopic reference in consistency with La Jolla neodymium. Chem. Geol. 168, 279–281.

Tolosa, I., Leblond, N., Copin-Montaigut, C., Marty, J.-C., de Mora, S., Prieur, L., 2003. Distribution of sterol and fatty alcohol biomarkers in particulate matter from the frontal structure of the Alboran Sea (S.W. Mediterranean Sea). Mar. Chem. 82, 161–183.

Toucanne, S., Jouet, G., Ducassou, E., Bassetti, M.-A., Dennielou, B., Minto'o, C.M.A., Lahmi, M., Touyet, N., Charlier, K., Lericolais, G., Mulder, T., 2012. A 130,000-year record of Levantine intermediate water flow variability in the Corsica Trough, western Mediterranean Sea. Quat. Sci. Rev. 33, 55–73. http://dx.doi.org/10.1016/j.quascirev.2011.11.020.

Tribovillard, N., Algeo, T.J., Lyons, T., Riboulleau, A., 2006. Trace metals as paleoredox and paleoproductivity proxies: an update. Chem. Geol. 232, 12–32. http://dx.doi.org/10.1016/j.chemgeo.2006.02.012.

Van der Weijden, C.H., 2002. Pitfalls of normalization of marine geochemical data using a common divisor. Mar. Geol. 184, 167–187.

Vance, D., Scrivner, A.E., Beney, P., Staubwasser, M., Henderson, G.M., Slowey, N.C., 2004. The use of foraminifera as a record of the past neodymium isotope composition of seawater. Paleoceanography 19, PA2009. http://dx.doi.org/10.1029/2003PA000957.

Voelker, A.H.L., Lebreiro, S.M., Schönfeld, J., Cacho, I., Erlenkeuser, H., Abrantes, F., 2006. Mediterranean outflow strengthening during northern hemisphere coolings: a salt source for the glacial Atlantic? Earth Planet. Sci. Lett. 245, 39–55.